UCRL-92429
PREPRINT

WIGGLE PLANE FOCUSING IN LINEAR WIGGLERS

E. T. Scharlemann

This paper was prepared for submittal to
Journal of Applied Physics

January 22, 1985

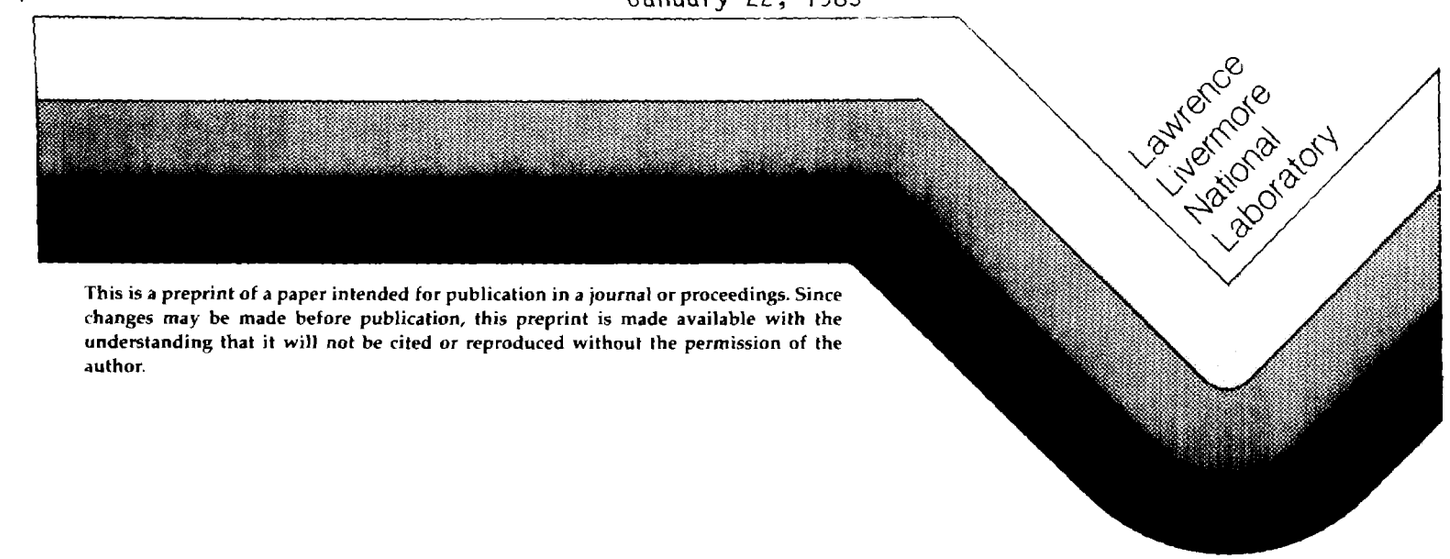

WIGGLE PLANE FOCUSING IN LINEAR WIGGLERS*

E. T. Scharlemann

January 22, 1985

Lawrence Livermore Laboratory
University of California
Livermore, CA 94550

ABSTRACT

In a free-electron laser with a long, linear wiggler, the external focusing required to keep the electron beam from dispersing can seriously degrade the performance of the laser. The transverse focusing modulates the longitudinal velocity of each electron, periodically and non-adiabatically changing the phase of the electron with respect to the electromagnetic wave. Phase changes of order unity over a betatron period can strongly detrap or debunch electrons and greatly reduce the gain of a linear wiggler amplifier. The modulation of the electron's longitudinal velocity can be prevented if focusing in the plane of the electron's wiggle motion is provided by parabolically curved magnet pole faces. The focusing and resonance effects of curved pole faces are analytically calculated and numerically confirmed. Numerical simulations of linear wiggler amplifiers are presented to illustrate the effect of the curved pole faces on amplifier performance.

*Performed jointly under the auspices of the U. S. Department of Energy by Lawrence Livermore National Laboratory under contract no. W-7408-ENG-48 and for the U. S. Department of Defense under DARPA, ARPA Order No. 4856, Program Code No. 3B10.

I. INTRODUCTION

The gain of a free-electron laser (FEL) depends critically on maintaining a precise phase relationship between the wiggle motion of the electrons and the electric field of the light. The electrons in a focused electron beam undergo transverse oscillations (betatron oscillations) in the focusing field. The oscillating transverse velocity can produce an oscillating longitudinal velocity, and thereby affect the gain. In a long wiggler some focusing is required; all electron beams have a non-zero spread in the angle at which individual electrons propagate (i.e., a non-zero emittance) and will eventually disperse in the absence of focusing.

In a helical wiggler, focusing in both transverse directions, x and y, is provided by the wiggler itself. The wiggler magnetic field necessarily increases away from the axis of the field; the spatial variation of the magnetic field focuses the electron beam. In a linear wiggler of conventional design, focusing is provided by the wiggler in only one of the transverse directions, the direction of the wiggler magnetic field. External focusing, usually provided by adding a quadrupole component to the field, is required in the other transverse direction (the wiggle plane).

The natural focusing of the wiggler has the well-known (but nonetheless curious) property that the longitudinal velocity of an electron, averaged over a wiggler period, is not modulated by the betatron oscillations of the electron. This property is described in detail in Sec. II. Natural wiggler focusing therefore does not affect the phase of an electron's wiggle motion with respect to the optical electric field. The only effect on the gain of

the FEL occurs because of the intrinsic spread of transverse velocities in the beam, and the only cure for that is to find a better quality beam. Quadrupole focusing (and most other forms of external focusing) introduces an additional problem; the longitudinal velocity, averaged over a wiggler period, is not constant throughout the betatron orbit of an electron. The phase between wiggle motion and electric field is periodically modulated by the betatron motion. In a high-gain constant-wiggler amplifier, where the gain is accompanied by physical bunching of the electron beam, the phase modulation can disperse the bunches, and reduce the gain. In a tapered-wiggler amplifier, where the gain is produced by the coherent deceleration of electrons trapped in ponderomotive potential wells,[1] the periodic phase modulation can detrap a significant fraction of the electrons.[2] The end result is that the difference in performance between a conventional linear wiggler with quadrupole focusing and the equivalent helical wiggler, for the same electron beam parameters, is much greater than would be expected from only the Bessel function field-particle coupling factor.[3]

Helical wigglers are, unfortunately, more difficult to build than linear wigglers; a helical wiggler with an adjustable taper would be extremely difficult to build. Furthermore, the linearly polarized light from a linear wiggler is very much easier to handle, at high output powers, than the helically polarized light from a helical wiggler. The purpose of this paper is to point out that a slight modification to the design of a linear wiggler can give the linear wiggler the focusing and resonance properties of a helical wiggler, with none of the technical difficulties of the helical wiggler. The modification consists of shaping the magnet pole faces with approximate

parabolic curvature transverse to the electron beam propagation direction [as done by Phillips[4] in 1960, in the Ubitron]. Parabolic curvature not only focuses the electron beam (as Phillips recognized) but also preserves the FEL resonance; the focusing and resonance properties are discussed in Sec. III. The importance of focusing by parabolic curvature rather than quadrupoles is illustrated with numerical simulations of a high-power, tapered-wiggler amplifier and of a lower-power, constant-wiggler amplifier. The simulation code and the results of a set of simulations with a) a helical wiggler, b) a linear wiggler with quadrupole focusing, and c) a linear wiggler with focusing by parabolic curvature, are described in Sec. IV.

The simulation code uses equations that describe particle motion averaged over a wiggler period. In order to ensure that the analytical treatment of focusing by parabolic curvature gives the correct focusing and resonance properties, we have done other simulations of the electron orbits in a wiggler without the average over a wiggler period. The results are described in Sec. V, and confirm the analytical derivations.

II. QUADRUPOLE FOCUSING IN A LINEAR WIGGLER

The magnetic field of an ideal linear wiggler is

$$\underset{\sim}{B} = \frac{mc^2}{e}\, b_0 \left[\hat{\underset{\sim}{y}} \cosh k_w y \cos k_w z - \hat{\underset{\sim}{z}} \sinh k_w y \sin k_w z\right] \quad , \tag{1}$$

where k_w is the wiggler wavenumber, and the electron beam propagates in the z-direction. The scaled field strength, b_0, has dimensions of cm^{-1} in cgs units. The wiggle motion is in the x-direction: the x - z plane is therefore the wiggle plane.

This field can be derived from a scalar potential

$$\underset{\sim}{b} \equiv \frac{e\underset{\sim}{B}}{mc^2} = - \underset{\sim}{\nabla}\chi \tag{2}$$

with

$$\chi = - \frac{b_0}{k_w} \sinh k_w y \cos k_w z \quad . \tag{3}$$

Because the field and potential do not depend on x, there is no focusing of the beam in the x-direction; in the y-direction, however, there is focusing that can be approximately described by the harmonic oscillator equation.[5] For the j^{th} electron

$$y_j'' \equiv \frac{d^2 y_j}{dz^2} = - k_{\beta y}^2 \, y_j \tag{4}$$

with

$$k_{\beta y} = \frac{b_0}{\sqrt{2}\,\gamma_j} \quad , \tag{5}$$

where γ_j is the electron's Lorentz factor.

The approximation used to obtain eq. (4) involves writing

$$\cosh k_w y \simeq 1 + \frac{k_w^2 y^2}{2} \quad . \tag{6}$$

In the same approximation, the wiggle motion is

$$x_j' = \frac{b_0}{\gamma k_w} \left(1 + \frac{k_w^2 y_j^2}{2} \right) \sin k_w z_j \; ; \tag{7}$$

the wiggle amplitude increases with y, as does B_y.

The wiggler focusing in y has the important property that the longitudinal (dimensionless) velocity $\beta_{\parallel}$ of an electron, averaged over a wiggle period, remains constant in the electron's betatron orbit. For $\gamma \gg 1$, $\beta_{\perp} \ll \beta_{\parallel}$ (and dropping the index j)

$$\beta_{\parallel} \approx 1 - \frac{1}{2\gamma^2} - \frac{\beta_{\perp}^2}{2} \tag{8}$$

but

$$\underset{\sim}{\beta}_{\perp} = \hat{\underset{\sim}{x}} \frac{b_0}{\gamma k_w}\left(1 + \frac{k_w^2 y^2}{2}\right) \sin k_w z + \hat{\underset{\sim}{y}}\ y' \quad . \tag{9}$$

where y' is the transverse betatron velocity of the electron. (Betatron motion in x is ignored here; we are only illustrating the properties of wiggler focusing.) From eq. (4), we can write

$$y = y_{\beta} \cos\left(k_{\beta y} z + \phi_y\right) \quad , \tag{10}$$

where ϕ_y is an arbitrary betatron phase, to obtain

$$\beta_{\perp}^2 = \frac{b_0^2}{\gamma^2 k_w^2}\left[1 + k_w^2 y_{\beta}^2 \cos^2\left(k_{\beta y} + \phi_{\beta y}\right)\right] \sin^2 k_w z$$

$$+ y_{\beta}^2 k_{\beta y}^2 \sin^2\left(k_{\beta} z + \phi_{\beta y}\right) \quad . \tag{11}$$

Averaging over a wiggle period ($\sin^2 k_w z \to 1/2$) and using eq. (5) for $k_{\beta y}$ yields

$$\overline{\beta_{\perp}^2} = \frac{b_0^2}{2\gamma^2 k_w^2}\left(1 + k_w^2 y_{\beta}^2\right) \quad . \tag{12}$$

This expression, and hence $\beta_{\parallel}$, are not modulated by the betatron motion.

It is important that $\beta_{\parallel}$ be constant in z so that an electron can remain nearly resonant with the ponderomotive potential well produced by the wiggler field plus the laser electromagnetic field. The phase of an electron in the ponderomotive potential well is often denoted by ψ, where[2]

$$\psi \equiv (k + k_w)z - \omega t + \phi \quad ; \tag{13}$$

k and ω are the wavenumber and angular frequency of the laser electromagnetic field, and ϕ is the phase of the electric field (see Sec. IV). Then, ignoring ϕ for the moment,

$$\frac{d\psi}{dz} = k + k_w - \frac{k}{\beta_{\parallel}} \tag{14}$$

$$\simeq k_w - \frac{k}{2\gamma^2} - \frac{k\overline{\beta_{\perp}^2}}{2} \quad ,$$

averaged over a wiggle period. If $\overline{\beta_{\perp}^2}$ is not constant, electrons are periodically pushed around in the ponderomotive well by their betatron motion.

This periodic pushing in ψ does occur if electron motion in the wiggle plane is confined by quadrupolar focusing, for which

$$x_0'' = - k_q^2 x_0$$

$$\text{with} \quad k_q^2 = q_0/\gamma \equiv \frac{e}{mc^2} Q_0/\gamma \quad . \tag{15}$$

Q_0 is the quadrupole strength (the field gradient), and x_0 is the slowly varying position of the guiding center of the electron's wiggle motion. The combination of guiding center harmonic motion with wiggle motion produces

$$x = x_\beta \cos (k_q z + \phi_q) - \frac{b_0}{\gamma k_w^2} \left(1 + \frac{k_w^2 y^2}{2}\right) \cos k_w z \quad . \tag{16}$$

Quadrupole focusing in x defocuses in y; instead of eq. (10), we have

$$y = y_\beta \cos (\tilde{k}_\beta z + \phi_y) \quad , \tag{17}$$

with

$$\tilde{k}_\beta^{\,2} = k_{\beta y}^{\,2} - k_q^{\,2} \quad . \tag{18}$$

For $\overline{\beta_\perp^{\,2}}$ we now find

$$\overline{\beta_\perp^{\,2}} = \frac{b_0^{\,2}}{2\gamma^2 k_w^{\,2}} \left[1 + k_w^{\,2} y_\beta^{\,2}\right] + \frac{k_q^{\,2}}{2} (x_\beta^{\,2} - y_\beta^{\,2})$$

$$+ \frac{k_q^{\,2}}{2} \left[y_\beta^{\,2} \sin 2 (\tilde{k}_\beta z + \phi_y) - x_\beta^{\,2} \sin 2 (k_q z + \phi_q)\right] . \tag{19}$$

The phases ϕ_y and ϕ_q are arbitrary so that the z-dependent term in the last square brackets of eq. (19) cannot, in general, be made to vanish. Therefore, $\overline{\beta_\perp^{\,2}}$ cannot be constant over a betatron period; the betatron motion of an electron changes its phase in the ponderomotive potential well, and can detrap the electron. A further discussion can be found in Ref. 2.

The importance of detrapping can be estimated by calculating the maximum deviation in ψ, over a betatron period in x, (no y motion) from Eqs. (14) and (19). At constant γ:

$$|\Delta\psi| \simeq \frac{k}{2} \cdot \frac{k_q^{\,2}}{2} \cdot x_\beta^{\,2} \cdot \frac{1}{k_q} = \frac{k k_q x_\beta^{\,2}}{4} \quad . \tag{20}$$

For the overall electron beam we can replace $k_q x_\beta^{\,2}$ by its rms value, to obtain

$$\langle \Delta\psi \rangle_{rms} \simeq \frac{k}{4} \varepsilon_x \quad , \tag{21}$$

where ε_x is the unnormalized, rms emittance in the x-direction:

$$\varepsilon_x \equiv k_q < x_\beta^2 >_{rms} \quad . \tag{22}$$

In order for detrapping by betatron motion in quadrupole focusing to be unimportant, we require

1) $\frac{k}{4} \varepsilon_x << 1$, or

2) L_w (the wiggler length) $<< \pi/k_q$.

III. PARABOLIC POLE FACES

The detrapping described in Sec. II occurs because the longitudinal velocity, $\beta_\parallel$, of an electron depends on the electron's phase in its betatron orbit in x; e.g., near $x = 0$ the transverse velocity of an electron is larger than near $|x| = x_\beta$, so the longitudinal velocity must be smaller. This variation in longitudinal velocity does not occur for betatron motion in y because the transverse velocity of the wiggle motion increases when the transverse velocity of betatron motion decreases, and vice versa.

We can circumvent the detrapping by betatron motion in x if the wiggle motion, hence B_y, increases with $|x|$ as well as with $|y|$; the $|x|$ dependence of B_y also provides focusing in x. In this section we demonstrate that this focusing, with no quadrupole focusing, keeps $\overline{\beta_\perp^2}$ constant and therefore does not affect the FEL resonance.

The focusing in x occurs for a different reason than the focusing in y described in Sec. II. The y-focusing arises from the cross-product of the wiggle motion x' [eq. (17)] with B_z [eq. (1)], averaged over a wiggler period. Both x' and B_z have a $\sin k_w z$ dependence; their product has a non-zero average value and produces an average force toward the x - z plane.

The focusing in x, if B_y increases with $|x|$, is a consequence of the larger acceleration by B_y, toward $x = 0$, at the outer extent (larger $|x|$) of the wiggle trajectory. The average force on an electron toward the y - z plane is non-zero because of the gradient of B_y in x.

The focusing force in x follows immediately from a standard analysis of motion in a rapidly oscillating force with a weak spatial gradient -- as found, for example, in Ref. 6. The effect of the x-gradient of B_y on focusing in y is not so straightforward; nor is a demonstration that $\overline{\beta_\perp^2}$ remains constant. Therefore, we reanalyze the focusing in both x and y. We can do this with the magnetic field obtained from

$$\chi = -\frac{b_0}{k_y} \cosh k_x x \sinh k_y y \cos k_w z \tag{23}$$

for which

$$\begin{aligned} b = \frac{b_0}{k_y} \Big\{ & \hat{x}\, k_x \sinh k_x x \sinh k_y y \cos k_w z \\ & + \hat{y}\, k_y \cosh k_x x \cosh k_y y \cos k_w z \\ & - \hat{z}\, k_w \cosh k_x x \sinh k_y y \sin k_w z \Big\} . \end{aligned} \tag{24}$$

This field is a vacuum solution of Maxwell's equations if

$$k_x^2 + k_y^2 = k_w^2 \quad . \tag{25}$$

In going from the conventional wiggler field of eq. (1) to eq. (24), we have effectively added a sextupole contribution: the difference of the transverse fields, for small $k_x x$ and $k_y y$, is

$$\Delta b_x = b_0 k_x^2 \, x \, y \tag{26}$$

$$\Delta b_y = b_0 \left(1 + \frac{k_x^2 x^2}{2} + \frac{k_y^2 y^2}{2}\right) - b_0 \left(1 + \frac{k_w^2 y^2}{2}\right)$$

$$= b_0 \frac{k_x^2}{2} (x^2 - y^2) \quad . \tag{27}$$

The difference field is the standard expression for a sextupole.

Sextupole fields are well known to give second-order focusing, with the transverse Lorentz force proportional to a second-order polynomial in x and y. At first glance the focusing in x appears fundamentally different from the focusing in y; however, as will be shown below, the cross term between wiggle motion and guiding center motion of an electron in x gives a harmonic (first order) focusing force on the electron's guiding center.

The harmonic focusing properties of an alternating sextupole component in a wiggler have previously been derived by Luccio and Krinsky[6] and Dattoli and Renieri,[7] in the context of transverse defocusing due to the finite width of magnet pole faces.

We are interested in $\overline{\beta_\perp^2}$ and the focusing averaged over a wiggle period, so we examine the focusing by using an averaging method. We assume the position r of an electron can be written

$$\underset{\sim}{r} = \underset{\sim}{r}_0 + \underset{\sim}{r}_1 \tag{28}$$

where $\underset{\sim}{r}_1' = (x_1', y_1', z_1')$ varies rapidly -- on a wiggler wavelength, and $\underset{\sim}{r}_0'$ is constant over a wiggler wavelength, but does vary over a betatron wavelength. $\underset{\sim}{r}_0$ is the guiding center position of the electron, and $\underset{\sim}{r}_1$ is the wiggle trajectory.

Furthermore, we will assume that the electron beam is small enough that $k_x x$ and $k_y y$ are small, and relativistic enough that $b_0/\gamma k_w$ is even smaller, so that an expansion in a small parameter is valid. If ϵ is the small parameter of the expansion, then $k_x x$ and $k_y y$ are $\mathcal{O}(\epsilon)$ and $b_0/\gamma k_w$ is $\mathcal{O}(\epsilon^m)$ for $m \geq 2$. The restriction on m merely ensures that $1/\gamma^2$ terms can be neglected with respect to $k_x^2 x^2$ or $k_y^2 y^2$ terms. For the simulations described below, $\epsilon \approx 0.1$ and $m = 2$. This ordering is appropriate for the high current, high emittance electron beam of an induction linear accelerator, but is <u>not</u> appropriate for an electron beam in a storage ring, where the focusing problem does not, in general, arise.

The equations of motion for an electron are

$$\ddot{x} = c\left[\dot{z}\frac{b_y}{\gamma} - \dot{y}\frac{b_z}{\gamma}\right] ,$$

$$\ddot{y} = c\left[\dot{x}\frac{b_z}{\gamma} - \dot{z}\frac{b_x}{\gamma}\right] , \tag{29}$$

$$\ddot{z} = c\left[\dot{y}\frac{b_x}{\gamma} - \dot{x}\frac{b_y}{\gamma}\right] ,$$

with b given by eq. (24). The dot denotes a time-derivative. The dominant terms in the wiggle motion come from

$$\ddot{x}_1 \approx c\dot{z}_0\frac{b_y}{\gamma} \tag{30}$$

from which we obtain

$$\dot{x}_1 = c\frac{b_0}{\gamma k_w}\left[1 + \frac{k_x^2 x_0^2}{2} + \frac{k_y^2 y_0^2}{2}\right]\sin k_w z \tag{31}$$

through $\mathcal{O}(\epsilon^4)$. Equation (31) describes the wiggle motion, which can be seen to increase with both x_0 and y_0.

The other component of the wiggle motion, $\dot{y}_1$, does not vanish; b_x is not zero so an equation analogous to eq. (30) could be written for $\dot{y}_1$. However, y_1 contributes to focusing and to $\overline{\beta_\perp^2}$ at much higher order than is retained in eq. (31), and so we neglect $\dot{y}_1$ altogether.

To evaluate the focusing, we write (including only the dominant terms)

$$\ddot{x}_0 = c\dot{z}_0 \frac{\overline{b_y}}{\gamma} \tag{32a}$$

$$\ddot{y}_0 = c \left[\overline{\dot{x}_1 \frac{b_z}{\gamma}} - \dot{z}_0 \frac{\overline{b_x}}{\gamma} \right] . \tag{32b}$$

The averages of b_x and b_y alone do not vanish because of the variation of b_x and b_y with x:

$$\begin{aligned} \ddot{x}_0 &= c^2 \dot{z}_0 \frac{b_0}{\gamma} \overline{\left[1 + \frac{k_x^2 (x_0 + x_1)^2}{2} + \frac{k_y^2 (y_0 + y_1)^2}{2} \right] \cos k_w z} \\ &\approx c^2 \dot{z}_0 \frac{b_0}{\gamma} k_x^2 x_0 \overline{x_1 \cos k_w z} \end{aligned} \tag{33}$$

or

$$\ddot{x}_0 \approx - \frac{c^2 b_0^2}{2\gamma^2 k_w^2} k_x^2 x_0 \equiv - c^2 k_{\beta x}^2 x_0 \tag{34}$$

after an average over a wiggle period.

In the same fashion, eq. (32b) yields

$$\ddot{y}_0 \approx - \frac{c^2 b_0^2}{2\gamma^2 k_w^2} k_y^2 y_0 \equiv - c^2 k_{\beta y}^2 y_0 \quad ; \tag{35}$$

the focusing in y has been decreased by the pole face design because of the $\dot{z}_0 \overline{b_x}/\gamma$ term in eq. (32b).

In order to evaluate $\overline{\beta_\perp^2}$ we need to connect $\ddot{x}_0$ and $\ddot{y}_0$ to x_0'' and y_0''. The only subtlety in making the connection can be seen from the identity

$$\ddot{x}_0 = (\dot{z})^2 x_0'' + \ddot{z} x_0' \quad ; \tag{36}$$

the $\ddot{z} x_0'$ term is not of higher order than the x_0'' term although the $(\dot{z})^2$ factor can be set to unity. The $\ddot{z} x_0'$ term does not, however, contribute to the focusing averaged over a wiggle period, so that we may write

$$\begin{aligned} x_0'' &= - k_{\beta x}^2 x_0 \quad , \\ y_0'' &= - k_{\beta y}^2 y_0 \quad . \end{aligned} \tag{37}$$

From Equations (37),

$$\begin{aligned} x_0 &= x_\beta \cos (k_{\beta x} z + \phi_x) \quad , \\ y_0 &= y_\beta \cos (k_{\beta y} z + \phi_y) \quad , \end{aligned} \tag{38}$$

and so

$$\begin{aligned} \dot{x}_0^2/c^2 &= k_{\beta x}^2 x_\beta^2 \sin^2(k_{\beta x} z + \phi_x) \\ \dot{y}_0^2/c^2 &= k_{\beta y}^2 y_\beta^2 \sin^2(k_{\beta y} z + \phi_y) \quad . \end{aligned} \tag{39}$$

For the wiggle motion

$$\overline{\dot{x}_1^2}/c = \frac{b_0^2}{2\gamma^2 k_w^2} \left[1 + k_x^2 x_0^2 + k_y^2 y_0^2\right] \quad ; \tag{40}$$

thus

$$\begin{aligned} \overline{\beta_\perp^2} &= \overline{\dot{x}_1^2}/c^2 + \dot{x}_0^2/c^2 + \dot{y}_0^2/c^2 \\ &= \frac{b_0^2}{2\gamma^2 k_w^2} \left[1 + k_x^2 x_\beta^2 + k_y^2 y_\beta^2\right] \quad . \end{aligned} \tag{41}$$

This is, indeed, constant for an individual electron over a betatron orbit.

This constant of the (averaged) motion was also derived by Dattoli and Renieri;[7] their concern was with a defocusing sextupole component.

We can get an approximate idea of the shape of the magnet pole face required to generate the focusing field of eq. (24) by the following argument. Assume the field is shaped by steel pole faces (as in a "hybrid" rare-earth cobalt and steel wiggler design)[8] and that the permeability $\mu \to \infty$ in the steel. At $\cos k_w z = 1$, the steel pole faces should then follow a curve of constant χ:

$$\cosh k_x x \sinh k_y y = C_0 \tag{42}$$

on the pole face.

The pole face then is described by the curve:

$$y(x) = \frac{1}{k_y} \sinh^{-1}\left(\frac{C_0}{\cosh k_x x}\right) , \tag{43}$$

or, approximately,

$$y(x) = \frac{C_0}{k_y}\left(1 - \frac{k_x^2 x^2}{2}\right) . \tag{44}$$

This form for $y(x)$ illustrates the approximately parabolic nature of the curvature.

The curve $y(x)$ for $k_x = k_y = k_w/\sqrt{2}$ is shown in Fig. 1; in this case, $k_{\beta x} = k_{\beta y}$ so the x focusing is sufficient to maintain a circular electron beam. It is interesting to note from Fig. 1 that only a small curvature to the pole faces is required to achieve a circular electron beam.

IV. NUMERICAL SIMULATIONS OF FEL PERFORMANCE WITH WIGGLE PLANE FOCUSING

The effect of quadrupolar focusing on the performance of a high-gain, tapered wiggler FEL was first realized when the LLNL 2D numerical simulation code FRED[2] was modified to include i) full betatron motion of the electrons, ii) the treatment of linear wigglers, and iii) quadrupole focusing in the wiggler plane. As mentioned in the introduction, the predicted performance of a linear wiggler was found to be much poorer than a helical wiggler for the same beam energy, current and emittance.

In its current version, the code follows 2000-4000 electrons within one ponderomotive potential well as they move in γ and ψ (longitudinal phase space). The equations that govern the motion in γ and ψ (averaged over a wiggler period) are slightly extended versions of those derived in Ref. 1:

$$\frac{d\gamma_i}{dz} = - e_s \frac{a_w f_B}{\gamma_i} \sin \psi_i \tag{45a}$$

$$\frac{d\theta_i}{dz} = k_w - \frac{k}{2\gamma_i^2} \left(1 + a_w^2 + \gamma_i^2 \beta_\perp^2{}_{,\beta} - 2 a_w f_B a_s \cos \psi_i + a_s^2\right) \tag{45b}$$

where a_w (r=0) $\equiv b_0/\sqrt{2}\, k_w$ for a linear wiggler, e_s is the scaled electric field strength, $e_s \equiv eE_s/\sqrt{2}\, mc^2$, $a_s \equiv e_s/k$, k is the wavenumber of the laser field, and $\beta_\perp^2{}_{,\beta}$ is the contribution of the betatron motion to $\beta_\perp^2$. In the code, the field quantities (including a_w) are all treated as functions of the electron's position (x_i, y_i, z_i), and $\beta_\perp^2{}_{,\beta}$ is evaluated in the electron's betatron orbit.

θ_i is the phase of the electron with respect to a plane electromagnetic wave, propagating with phase velocity equal to c. In terms of the phase in the ponderomotive potential well, ψ_i, and the phase of the electric field ϕ [see below, eq. (51)]

$$\theta_i \equiv \psi_i - \phi \quad . \tag{46}$$

The quantity f_B in eq. (45) is a difference of Bessel functions[3] and differs from unity for a linear wiggler as a consequence of averaging over a wiggler period. For a helical wiggler, $f_B = 1$; for a linear wiggler

$$f_B \equiv J_0(\xi) - J_1(\xi) \tag{47}$$

where

$$\xi \equiv \frac{a_w^2}{2(1+a_w^2)} \quad .$$

The equations for the transverse motion are of the form

$$\begin{aligned} x_i'' &= - k_{\beta x}^2 \, x_i \\ y_i'' &= - k_{\beta y}^2 \, y_i \quad , \end{aligned} \tag{48}$$

with $k_{\beta x}$ and $k_{\beta y}$ functions of z and γ in ways dependent on the specific kind of focusing assumed. For the scheme described in Section III, $k_{\beta x}$ and $k_{\beta y}$ are given by Eqs. (34) and (35). For quadrupole focusing in the wiggle plane (hence defocusing in y) $k_{\beta x} = k_q$ from eq. (15) and $k_{\beta y} = \tilde{k}_\beta$ from eq. (18). For a helical wiggler

$$k_{\beta x} = k_{\beta y} = \frac{b_0}{\sqrt{2}\gamma} \quad . \tag{49}$$

The electron betatron motion is fully 3-dimensional. The laser field, however, is assumed to be 2-dimensional; for the simulations described here, the laser field is cylindrically symmetric, and the two dimensions are r and z.

The field is solved in the paraxial approximation.[10] The electric field -- linearly polarized, for a linear wiggler -- is written

$$E_x(x,y,z,t) = R_e \left[\mathcal{E}(x,y,z)\, e^{i\,(k\,z\,-\,\omega\,t)} \right] \quad , \tag{50}$$

where $\mathcal{E}$ is a slowly varying, complex electric field amplitude: the equation

$$\mathcal{E} \equiv |\mathcal{E}|\, e^{i\phi} \tag{51}$$

defines ϕ, the phase of the electric field. The code can also simulate a helical wiggler FEL; the modifications to the field equations are straightforward.

With the slowly-varying amplitude and phase approximation, the wave equation becomes

$$\begin{aligned} \nabla^2 E_x - \frac{1}{c^2}\,\frac{\partial^2 E_x}{\partial t^2} &\simeq \frac{1}{2}\left[e^{i(k\,z\,-\,\omega\,t)}\,\left(2ik\,\frac{\partial}{\partial z} + \nabla_\perp^2\right)\mathcal{E} + \text{c.c.} \right] \\ &= \frac{4\pi}{c^2}\,\frac{\partial}{\partial t}\,J_x \quad . \end{aligned} \tag{52}$$

In cylindrical symmetry

$$\nabla_\perp^2 = \frac{1}{r}\,\frac{\partial}{\partial r}\,r\,\frac{\partial}{\partial r} \quad . \tag{53}$$

For the source term - the right-hand side of eq. (52) - we assume that only the Fourier component of J_x proportional to $e^{i(k\,z\,-\,\omega t)}$ contributes to the field evolution. Implicit is the approximation that the field changes little over many optical wavelengths.

Defining,

$$\frac{e\mathcal{E}}{\sqrt{2}mc^2} \equiv e_1 + i\,e_2 = e_s\, e^{i\phi} \tag{54}$$

(the factor of $\sqrt{2}$ ensures that e_1 and e_2 refer to rms values), and writing

$$J_x\,(x,y,z) = -\,e \sum_i v_{x_i}\,\delta(x - x_i)\,\delta(y - y_i)\,\delta(z - z_i) \tag{55}$$

with

$$v_{xi} = c \frac{\sqrt{2} a_w}{\gamma_i} \cos k_w z_i \quad , \tag{56}$$

eq. (52) becomes[3]

$$(2ik \frac{\partial}{\partial z} + \nabla_\perp^2) (e_i + ie_2) \simeq \frac{4\pi i \omega e \, a_w f_B}{mc^4} \frac{I}{N} \sum_i \frac{e^{-i\theta_i}}{\gamma_i} \delta(x - x_i)\delta(y - y_i). \tag{57}$$

Here I is the beam current and N the number of simulation particles; I/N is therefore the current per particle. The field quantities e_1 and e_2 are both functions of x, y, and z.

To solve eq. (57) numerically, we integrate both sides over radial zones of width Δr(in general, Δr varies with r). Then, at a radial grid point,

$$(2ik \frac{\partial}{\partial z} + \nabla_\perp^2) (e_i + ie_2) \simeq \frac{2i\omega e \, a_w f_B}{mc^4} \frac{I}{N} \frac{1}{r\Delta r} \sum_i \frac{e^{-i\theta_i}}{\gamma_i} \tag{58}$$

where now the sum is only over the particles lying within the radial zone Δr around the grid point.

Equation (58) is solved in FRED using a finite element method, which permits a unique weighting of particles to radial grid points.

We first present the results of three simulations for an FEL with a 25 m wiggler driven by a 50 MeV induction linac. The three simulations differ only by type of wiggler - a) helical, b) linear with wiggle plane focusing due to parabolic pole faces and c) linear with external quadrupole focusing. In all three cases, the wiggler is tapered in a_w according to the usual self-design procedure:[1,2] a design electron, in a circular orbit at r_{design}, is

maintained at a fixed $\psi_r = 0.35$, by changing a_w as the electron is decelerated. The other parameters for all three runs are listed in Table I.

In all three cases, the beam waist occurs 0.5 Rayleigh ranges before the wiggler; the entering laser beam is diverging (we have found the FEL amplifier to perform better for a diverging input beam than for a converging input beam, for reasons beyond the scope of this paper). Figure 2 shows the calculated laser power as a function of z in the wiggler; the third case (curve c) with quadrupole focusing sufficient to keep the electron beam circular, performs less than a third as well as the helical wiggler (curve a), and less than half as well as the linear wiggler with parabolic pole faces (curve b). The reason for the poor performance can be seen in Fig. 3; this is a plot of trapped ($-\pi < \psi < \pi$) electron fraction as a function of z for the three cases. The linear wiggler with quadrupole focusing shows strong, steady detrapping throughout the wiggler, with a very small final trapping fraction. The linear wiggler with parabolic pole faces did not perform quite as well as the helical wiggler; the Bessel function factor ($f_B \simeq 0.83$ initially) readily explains the difference.

In the second set of simulations, we illustrate the effect of quadrupole focusing on exponential gain, for a shorter wiggler (5 meters) driven by a 50 MeV induction linac. The properties of the electron and laser beams are those listed in Table I, except the input laser power, P_{in}, is only 1 MW. In these cases the laser beam is focused at the entrance to the wiggler. The wiggler is untapered. Fig. 4 shows the resulting laser power as a function of z. The plot is semi-logarithmic to permit comparison of the exponential gain. Curve (b) of Fig. 4 illustrates exponential gain in linear wiggler with parabolic pole faces -- the gain of 5.4 dB m^{-1} is less than for

the helical wiggler (6.7 dB m^{-1}) by roughly the Bessel function factor. The gain in a linear wiggler with quadrupole focusing, curve (c) of Fig. 4 is seen to drop abruptly at 3 m, or roughly a quarter of a betatron wavelength. The initial gain is ~ 5.4 dB m^{-1}, as in Fig. 4b, but as the electron bunching is dispersed by the betatron motion of the electrons, the gain drops to 3 dB m^{-1}. The output power after 5 m is an order of magnitude less than for a helical wiggler, largely because of the debunching past 3 m.

V. NUMERICAL ORBIT CALCULATIONS

The simulations described in Sec. V use the transverse equations of motion averaged over a wiggler period, eqs. (45a) and (45b), to calculate the electron trajectories. The focusing and resonance properties of curved pole faces are therefore built into the simulations, rather than appearing from the exact solution to eq. (29). It is a simple matter to integrate the exact equations of motion in the wiggler, eq. (29), to verify the properties derived in Sec. III. We have done so, and present examples of the results here. It is not a simple matter to incorporate the exact transport equations into our FEL simulations. The FEL simulations utilize the averaged equations derived in Ref. (1), and only the average $\gamma^2\beta_\perp^2$ appears in the $d\psi/dz$ equation, eq. (45b). A careful numerical average of the exact trajectory for each electron would therefore be needed.

In this section we examine the betatron orbits and the average $\beta_\parallel$ obtained by integrating eq. (29) with the magnetic field of eq. (24). For the parameters of the third simulation described in Sec. V, eqs. (34) and (35) predict a betatron wavelength of 8.8 meters. Figure 5 shows the orbits,

projected on the x-y plane, of electrons with $\gamma = 100$, in a constant wiggler field of 2.4 kG. The calculation is carried out for half the predicted betatron wavelength, i.e., 4.4 m. The nine plots in the figure are for particles initialized in orbits that should be circular (first column), elliptical (second column), or linear in y (last column), at maximum betatron radii of 0.1 cm (top row), 0.2 cm (middle row), or 0.3 cm (bottom row). It is clear that the qualitative properties of the orbits agree with analytical calculation (e.g., those orbits that should be circular are, indeed, circular, with no unexpected transport resonances).

For the FEL resonance, the average of $\gamma^2\beta_\perp^2$, and hence the average of $\beta_\parallel$, over a wiggler period is expected to be constant, eq. (41). We illustrate this property of the orbits for the outermost three electrons [the bottom row in Fig. 5] in Fig. 6, where we plot k (the laser wavenumber) times the departure of z(t) from a straight line over the betatron period of the calculation. The plotted quantity is very nearly $\Delta\psi$ (eq. 13) for a resonant electron, <u>without</u> an average over a wiggler period, but sampled once per wiggler period to remove the rapid wiggle motion. The shift in ψ due to betatron motion is tiny: less than $2.4 \cdot 10^{-3}$ radians in all cases.

In demonstrating that $\beta_\parallel$ is constant over a betatron orbit, it is necessary to choose the right endpoints for the orbit integrations. The proper endpoints can be found from the analytical expression for the perturbations to z(t):

$$z_1(t) = \dot{x}_0 \frac{b_0 k_y}{\gamma k_w^2} \cos k_w z + \frac{a_w^2}{\gamma^2} \frac{k_y^2}{8k_w^3} \sin 2 k_w z \quad . \tag{59}$$

Both terms are rapidly oscillating, and average to zero over many wiggler periods, but vanish together at

$$k_w z = (2n + 1)\frac{\pi}{2}\ ,\ n = 0,1\ \ldots; \tag{60}$$

the endpoints must be chosen at values of z that satisfy condition (60). Endpoints which satisfy that condition were used in producing Fig. 6.

Fig. 7 is a similar plot when external quadrupole focusing is used to keep the beam circular -- in this case, to give the particle orbits the same eccentricity as previously. Strong betatron modulation, corresponding to a shift in optical phase of $\mathscr{O}(1)$ radians, is apparent. The lack of this modulation is the reason that curved pole faces should produce a more efficient FEL.

VI. SUMMARY

Periodic sextupole focusing, easily provided by curved magnet pole faces in the wiggler, can greatly enhance the performance of a free-electron laser amplifier. Unlike quadrupole focusing, the periodic sextupole focusing does not affect the relative phase of an electron's wiggle motion and the laser electric field; periodic sextupole focusing therefore permits an electron beam to bunch coherently more readily than does quadrupole focusing. We have derived the resonance properties of periodic sextupole focusing, confirmed them with numerical simulations, and illustrated their importance with two simulations of induction-linac driven FELs.

I am happy to acknowledge useful conversations with W. M. Fawley, K. Halbach, V. K. Neil, D. Prosnitz, A. M. Sessler and J. S. Wurtele. The simulation code FRED is co-authored by W. M. Fawley.

REFERENCES

1. N. M. Kroll, P. L. Morton, and M. N. Rosenbluth, IEEE Journal Quantum Electronics 17, 1436 (1981).
2. W. M. Fawley, D. Prosnitz, and E. T. Scharlemann, Phys. Rev. A, 30, 2472 (1984)
3. W. B. Colson, IEEE Journal Quantum Electronics, 17, 1417 (1981).
4. R. M. Phillips, IRE Trans. on Electron Devices, 7, 231 (1960).
5. V. K. Neil, SRI Tech. Rept. JSR-79-10 (1979); see also C. M. Tang, NRL Memorandum 4820 (1982).
6. A. Luccio and S. Krinsky, Free-Electron Generators of Coherent Radiation, S. F. Jacobs, G. T. Moore, H. S. Pilloff, M. Sargent III, M. O. Scully, and R. Spitzer, eds. (Physics of Quantum Electronics, Vol. 8), Addison-Wesley, 1982, p. 181.
7. G. Dattoli and A. Renieri, "Experimental and Theoretical Aspects of the Free Electron Laser," to be published.
8. K. Halbach, Journal de Physique, Suppl. C1 44, 211 (1983) (Bendor Free Electron Laser Conference.)
9. L. D. Landau and E. M. Lifshitz, Mechanics (Pergamon, NY, 1976) p. 93.
10. J. H. Marburger, Prog. Quant. Electronics, 4, 35 (1975).

FIGURE CAPTIONS

Fig. 1: An illustration of curvature of the steel pole faces in a hybrid wiggler required to keep the electron beam circular; i.e., $k_{\beta x} = k_{\beta y}$.

Fig. 2: Laser power as a function of distance z in the wigglers for the three cases discussed in the text: a) a helical wiggler, b) a linear wiggler with parabolically curved pole faces, and c) a linear wiggler with quadrupole focusing strong enough to keep the electron beam circular. The simulation parameters are listed in Table I.

Fig. 3: Fraction of electrons trapped in the ponderomotive well, as a function of z, for the three cases of Fig. 2.

Fig. 4: Laser power as a function of z for 1 MW input power with an untapered wiggler. The three cases are the three wiggler types of Fig. 2.

Fig. 5: Exact x-y electron orbits for nine electrons in a linear, untapered wiggler with curved pole faces. The electron orbits were followed for half a betatron period in z; plotted here are the projections of the trajectories onto the x-y plane. The orbit types are circular (left column), elliptical (center column) and linear in y (right column); the maximum betatron radii are 0.1 cm (top row), 0.2 cm (center row) and 0.3 cm (bottom row).

Fig. 6: Deviation of the longitudinal position of the three electrons in the bottom row of Fig. 5 from an exactly straight line (constant $\beta_{\parallel}$) orbit, measured in units of radians of optical phase.

Fig. 7: The same as Fig. 6 for electrons maintained in their orbits by strong quadrupole focusing.

Table I Tapered Wiggler Amplifier Simulation parameters

$\gamma = 100$	(electron Lorentz factor)
$\epsilon_N = 0.14$ rad cm	(normalized edge emittance for a parabolic beam profile).
$P_{in} = 800$ MW	(peak laser input power)
$I = 2$ kA	(electron beam current)
$\omega_0 = 0.35$ cm	(input laser beam waist)
$\lambda_w = 8$ cm	(wiggler wavelength)
$\lambda_s = 10.6$ μm	(signal wavelength).

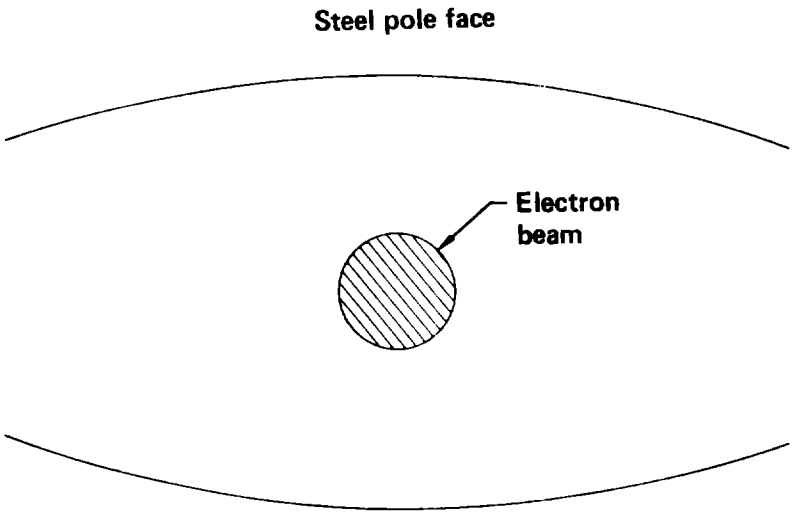

Figure 1

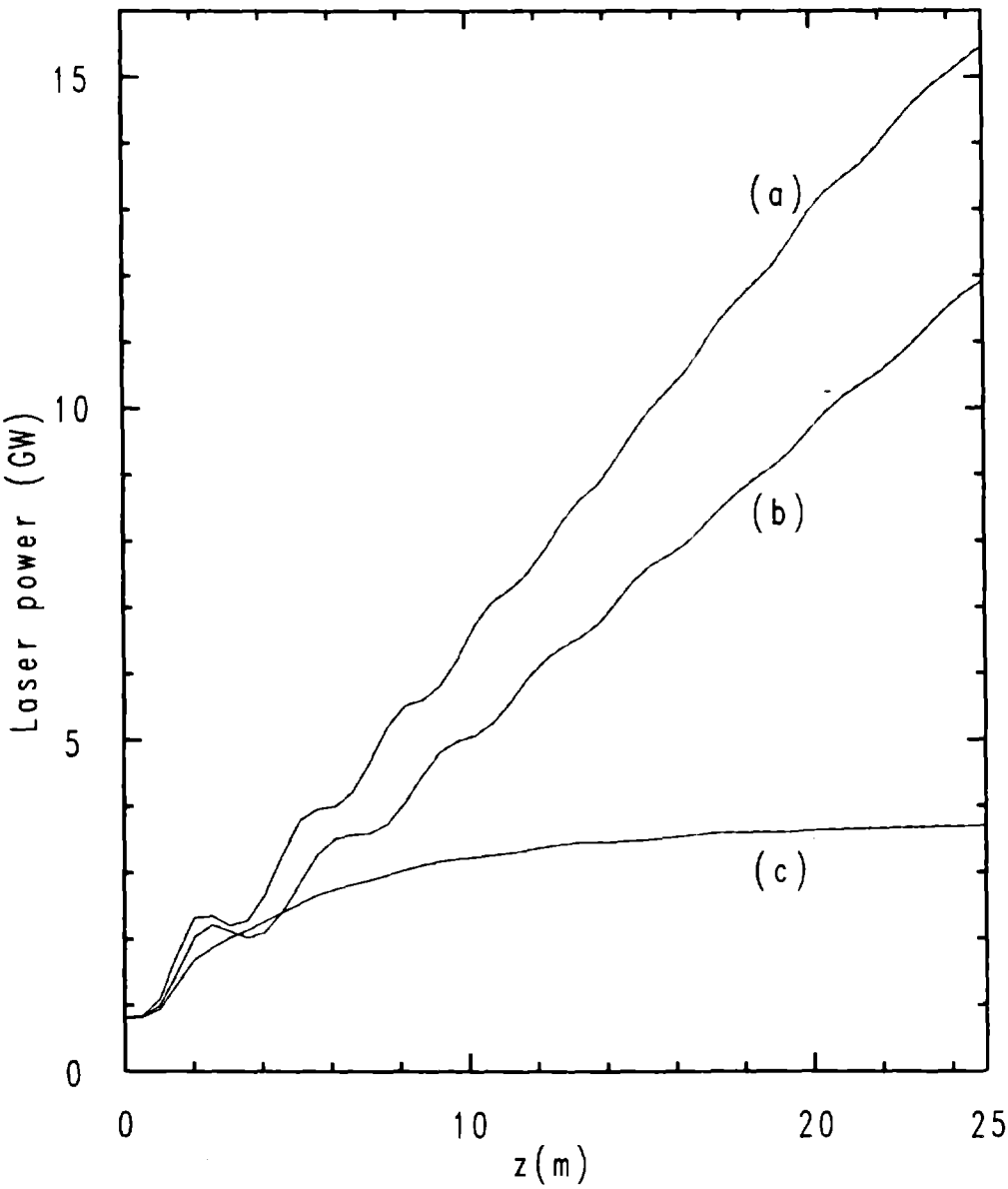

Figure 2

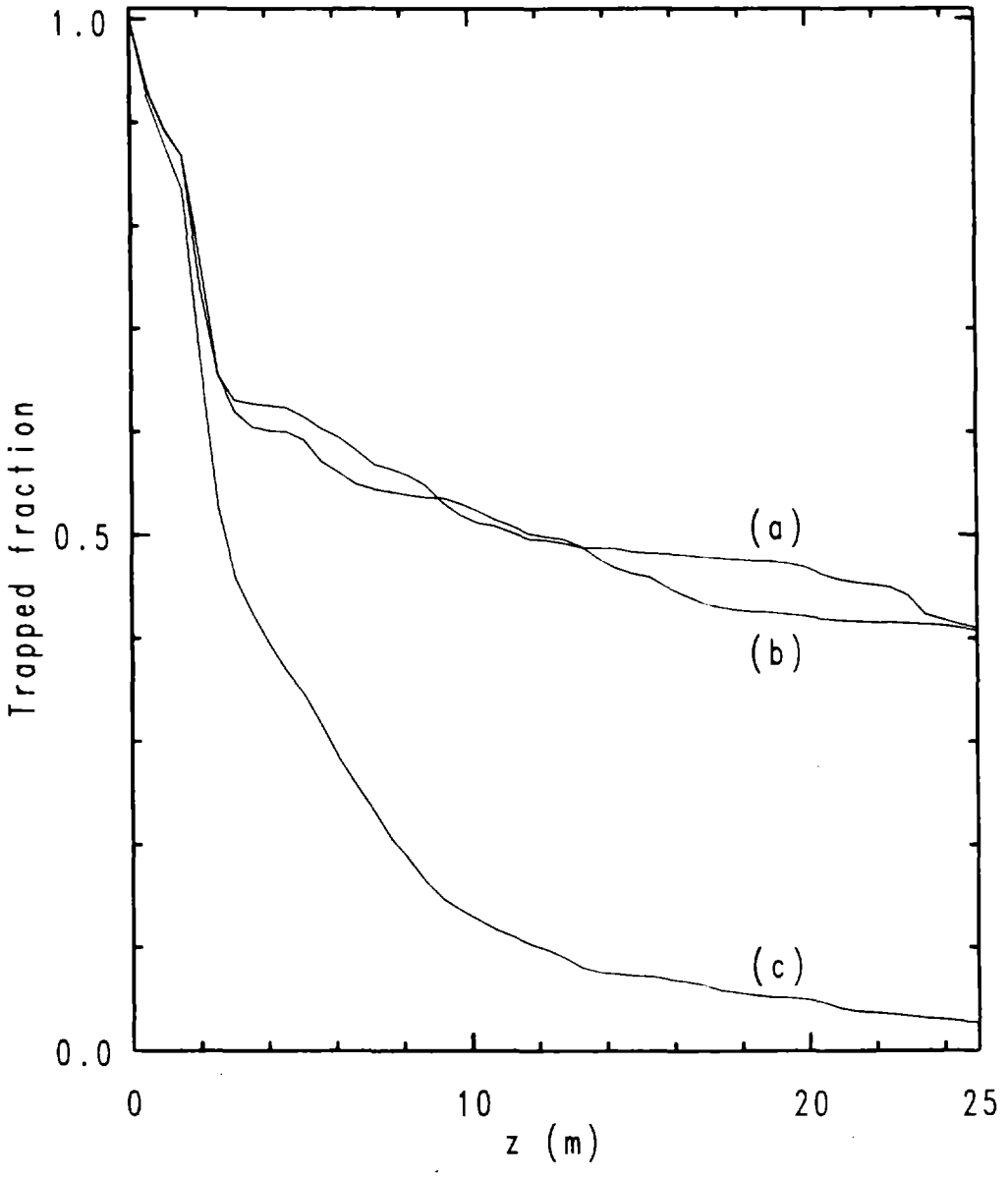

Figure 3

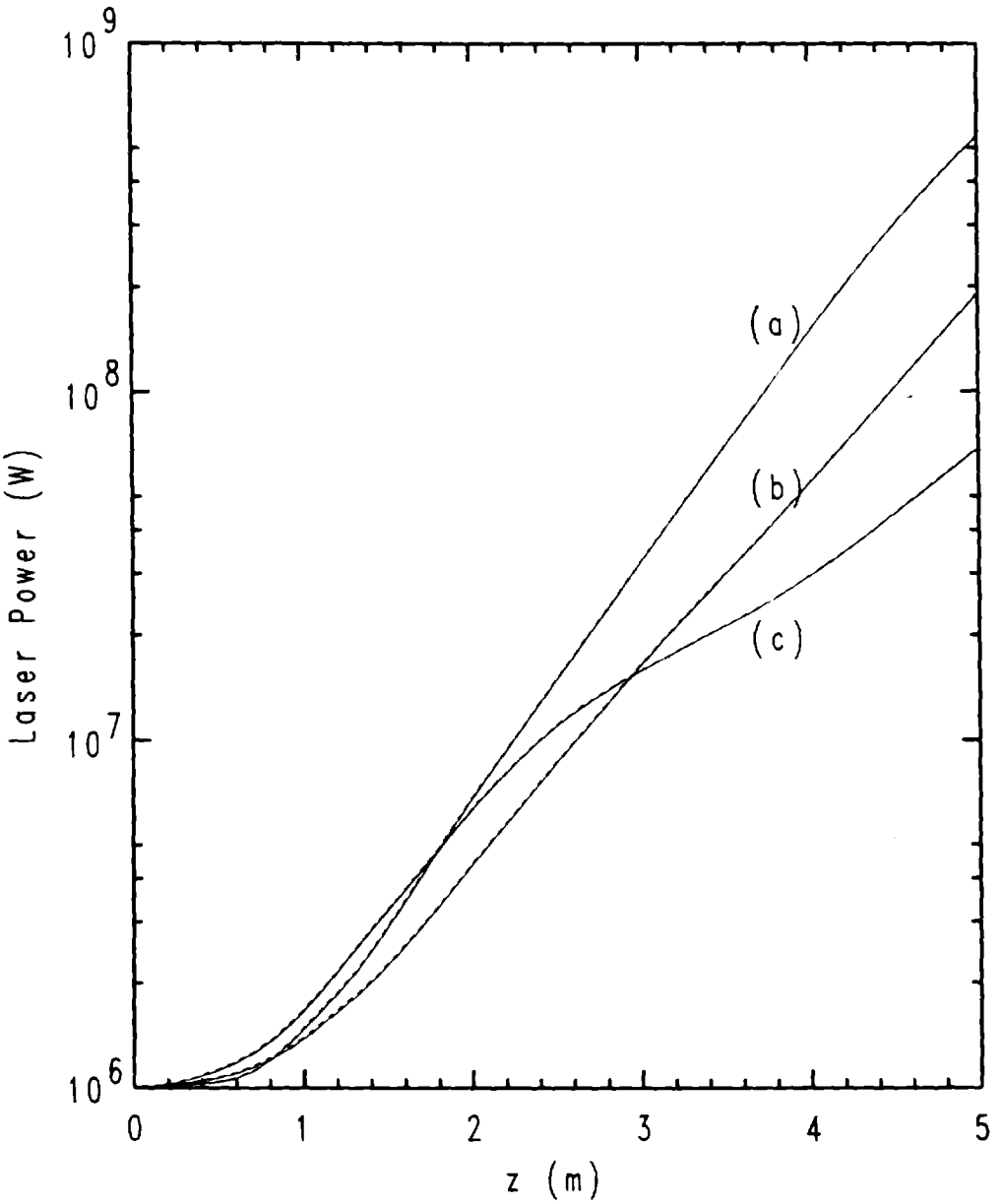

Figure 4

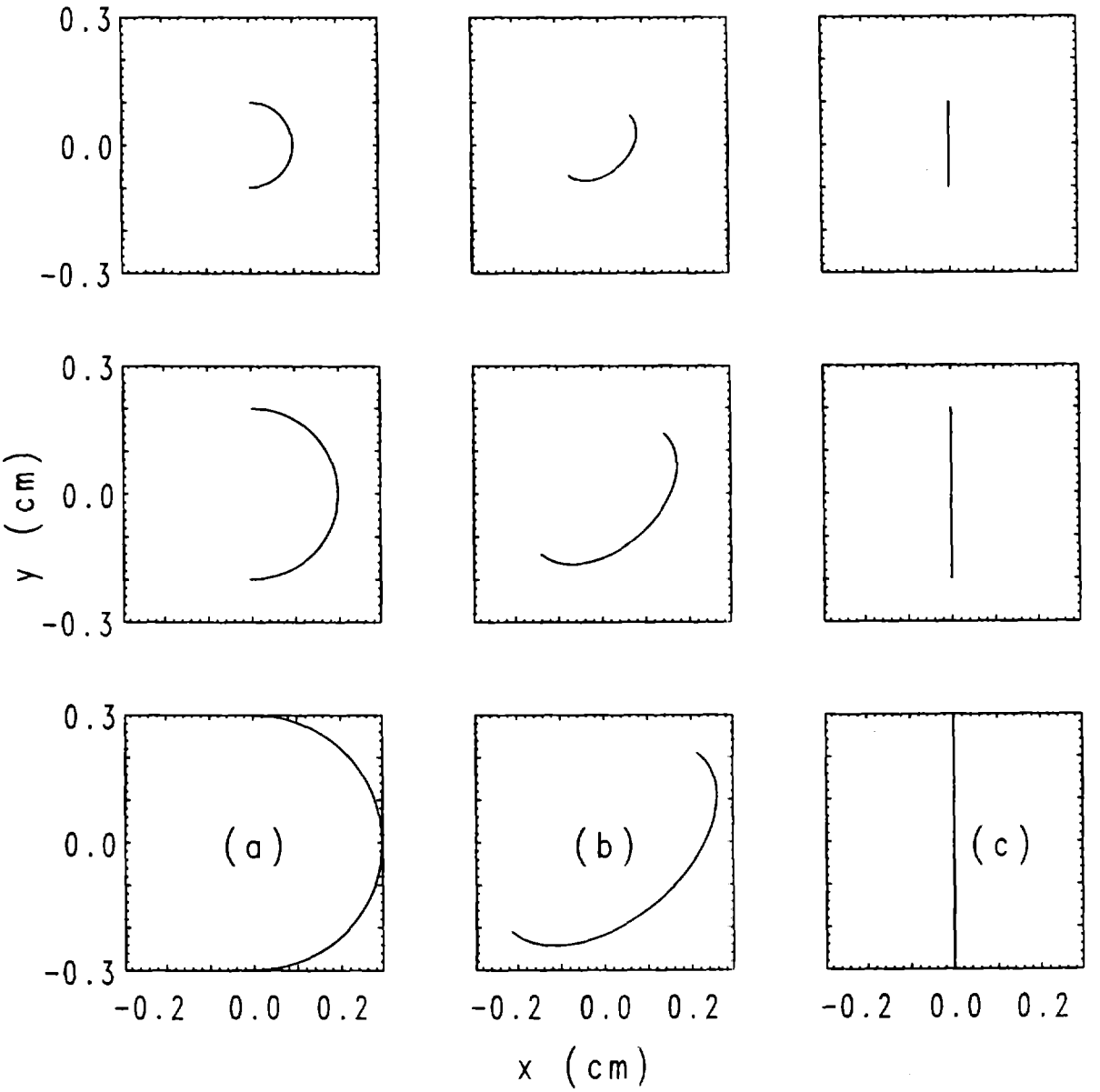

Figure 5

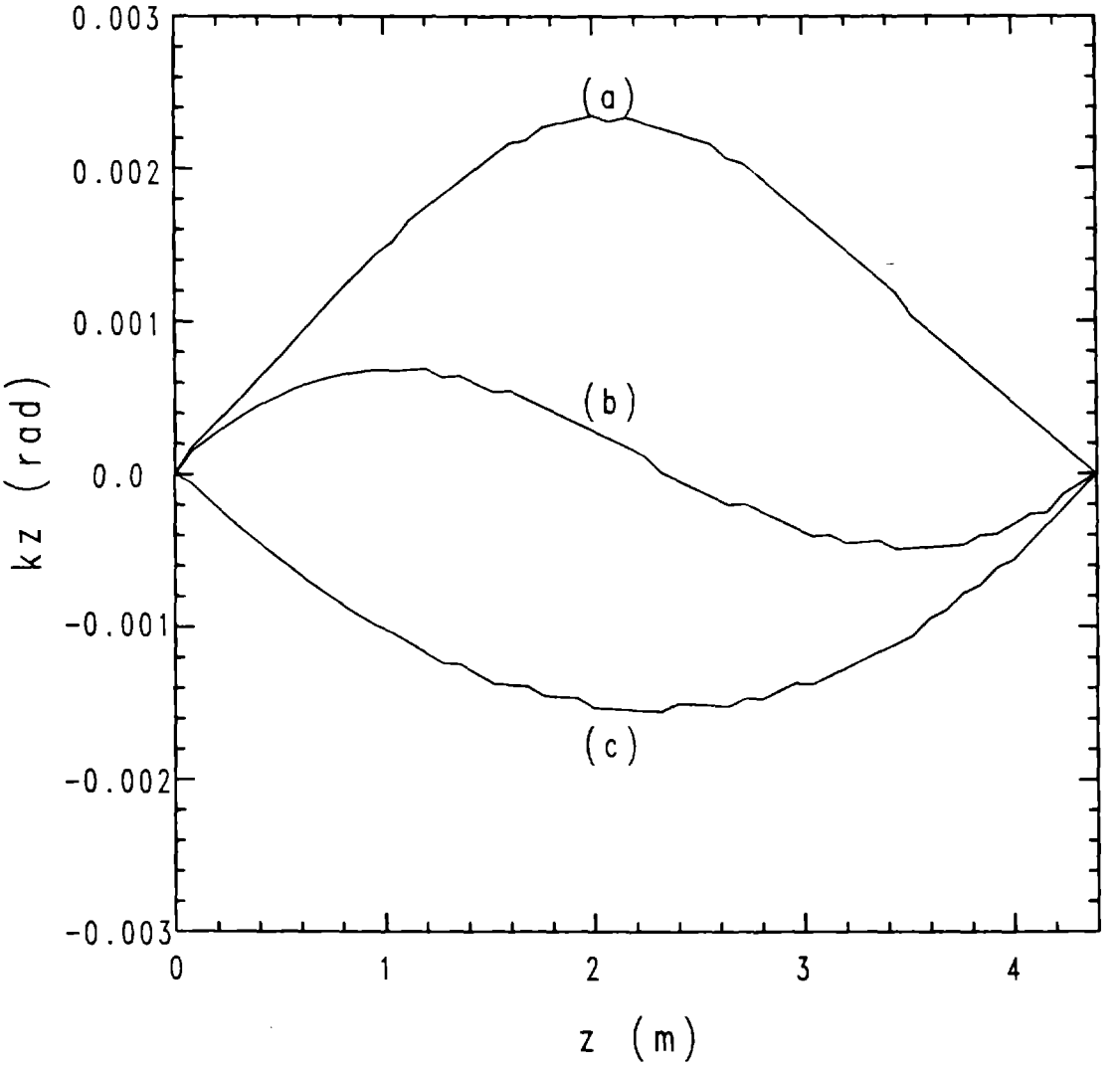

Figure 6

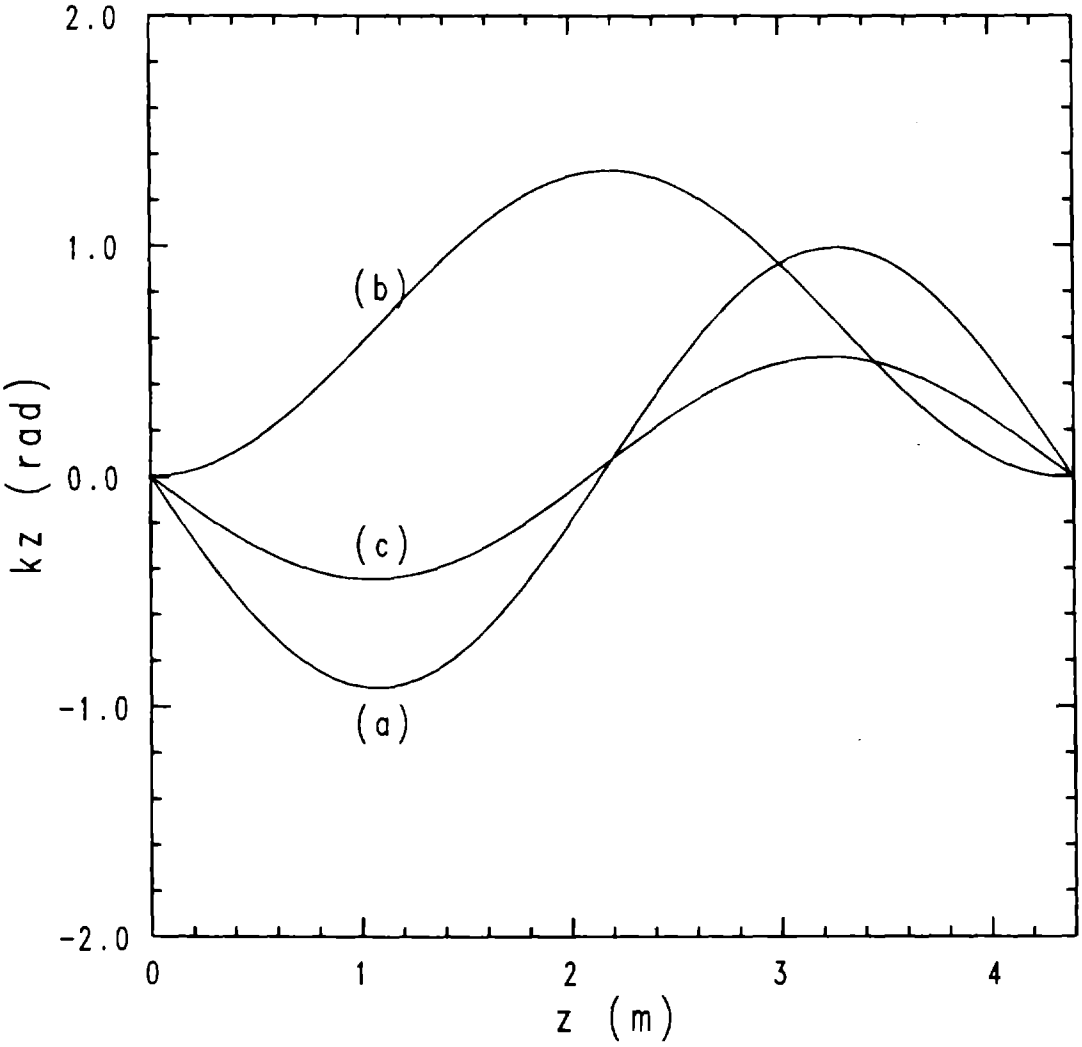

Figure 7